AIP Advances

W thickness dependence of spin Hall effect for (W/Hf)-multilayer electrode/CoFeB/MgO systems with flat and highly (100) oriented MgO layer

Cite as: AIP Advances **11**, 025007 (2021); https://doi.org/10.1063/9.0000011
Submitted: 30 September 2020 . Accepted: 16 January 2021 . Published Online: 04 February 2021

Yoshiaki Saito, Nobuki Tezuka, Shoji Ikeda, and Tetsuo Endoh

View Online Export Citation CrossMark

AIP Advances
Fluids and Plasmas Collection
READ NOW

© 2021 Author(s).

W thickness dependence of spin Hall effect for (W/Hf)-multilayer electrode/CoFeB/MgO systems with flat and highly (100) oriented MgO layer

Cite as: AIP Advances 11, 025007 (2021); doi: 10.1063/9.0000011
Presented: 6 November 2020 • Submitted: 30 September 2020 •
Accepted: 16 January 2021 • Published Online: 4 February 2021

View Online Export Citation CrossMark

Yoshiaki Saito,[1,a)] Nobuki Tezuka,[2,3] Shoji Ikeda,[1,3,4,5] and Tetsuo Endoh[1,3,4,5,6]

AFFILIATIONS

[1]Center for Innovative Integrated Electronic Systems, Tohoku University, Sendai 980-0845, Japan
[2]Department of Materials Science, Graduate School of Engineering, Tohoku University, Sendai 980-8579, Japan
[3]Center for Spintronics Research Network, Tohoku University, Sendai 980-8577, Japan
[4]Center for Science and Innovation in Spintronics, Tohoku University, Sendai 980-8577, Japan
[5]Research Institute of Electrical Communication, Tohoku University, Sendai 980-8577, Japan
[6]Department of Electrical Engineering, Graduate School of Engineering, Tohoku University, Sendai 980-8579, Japan

Note: This paper was presented at the 65th Annual Conference on Magnetism and Magnetic Materials.
[a)]**Author to whom correspondence should be addressed:** ysaito@cies.tohoku.ac.jp

ABSTRACT

We investigated spin-Hall effect (SHE) and degree of MgO (100) orientation in artificially synthesized (W/Hf)-multilayer/CoFeB/MgO systems with various W thicknesses. We found that the artificially synthesized multilayer systems can enhance the spin-Hall effect and control the value of spin diffusion length. We observed a maximum magnitude in both spin-Hall angle and spin-Hall conductivity as a function of W thickness in W/Hf-multilayer systems, and found that the values of spin-Hall conductivity are larger than that for β-phase W. In addition, a more highly oriented MgO (100) texture on CoFeB is obtained for (W/Hf)-multilayer systems prepared under low-Ar-pressure condition, which would be suitable for preparation of magnetic tunnel junctions with high tunnel magnetoresistance properties on (W/Hf)-multilayer heavy metal electrode. These results suggest that the artificially synthesized multilayer system is one of the avenues for realizing spin devices using spin-orbit torque.

© 2021 Author(s). All article content, except where otherwise noted, is licensed under a Creative Commons Attribution (CC BY) license (http://creativecommons.org/licenses/by/4.0/). https://doi.org/10.1063/9.0000011

I. INTRODUCTION

Current-induced spin-orbit torque (SOT) originating from the spin-Hall effect (SHE) in heavy metal/ferromagnet (HM/FM) systems has attracted attention due to their potential for application to SOT magnetoresistive random access memory (SOT-MRAM), skyrmion and domain wall devices.[1–18] Study of HM materials as well as HM/FM interfaces with larger spin-orbit coupling is being actively carried out because of allowing a larger amount of spin current (J_s) to be generated for manipulating the nano magneto when flowing the write charge current (J_C) through the HM layers. For the application to a large-scale integration, the efficient SOT operation (absolute value of high spin Hall angle $|\theta_{SH}|$) in low resistivity (ρ_{xx}) HM is necessary.[19–21] The low $|\theta_{SH}|$ and high ρ_{xx} lead to an undesirably large energy dissipation, delay in speed, and large voltage drop during current flow in HMs. Magnitudes of the $|\theta_{SH}| = |J_S/J_C|$ have been determined for various HMs by measuring the spin-Hall magnetoresistance (SMR) and spin torque ferromagnetic resonance (ST-FMR)[19–26] and by other means. Due to the extensive efforts, the efficiency of present SOT operations, that is, $|\theta_{SH}|$ becomes larger day by day, however, almost all HMs have large resistivity. For example,

© Author(s) 2021

β-phase W (β-W) has a relatively large $|\theta_{SH}|$ of approximately 0.2 - 0.3, however, β-W have a very high ρ_{xx}.[1,12,21,22,25–28] The magnitude of $|\theta_{SH}|$ for both intrinsic and extrinsic (side jump mechanism) terms is proportional to the magnitude of ρ_{xx} value ($|\theta_{SH}| \sim \sigma_{SH}\,\rho_{xx}$[27,28]), where σ_{SH} is spin Hall conductivity. Therefore, increase in the magnitude of σ_{SH} is important from the application point of view.[21] Recently, we observed that large magnitude of σ_{SH} and enhancement of perpendicular magnetic anisotropy in (W (t_W)/Hf (t_{Hf}))-multilayer/CoFeB/MgO systems with $t_W = t_{Hf}$ = 0.35 nm and 0.7 nm compare to β-W/CoFeB/MgO system.[21] In the previous work, we also found magnitude of σ_{SH} for (W (0.7)/Hf (0.7))-multilayer system is larger than that for (W (0.35)/Hf (0.35))-multilayer system. Therefore, when the film thickness ratio between W and Hf is optimized, further increase of σ_{SH} is expected in the (W/Hf)-multilayer system.

In this paper, we investigated W thickness dependence of σ_{SH}, θ_{SH}, ρ_{xx} and spin diffusion length (λ_S) in amorphous (W (t_W)/Hf (0.35))-multilayer/CoFeB/MgO systems with various t_W and evaluated the degree of MgO (100) orientation on the (W/Hf)-multilayer HM electrode.

II. EXPERIMENTS

We prepared Ta(0.5)/artificially-synthesized (W(t_W)/Hf(0.35))$_n$ multilayer (t_{HM})/CoFeB(t_{CoFeB})/MgO(1.0)/Ta(1) (n: repetition number) systems with various HM thicknesses (t_{HM}) on high resistive Si substrates. The sputtering Ar gas pressure (P_{Ar}) for W in W/Hf multilayers employed 2.55 Pa (high-Ar-pressure condition) and 0.39 Pa (low-Ar-pressure condition), which are β- and a-phases preparation conditions in W deposition, respectively, as reported previously.[19] The (W (t_W)/Hf (0.35))-multilayer systems have amorphous structure as described in Ref. 21. These systems with various t_{HM} (= 1.1~8.4 nm) are patterned into the microscale Hall bar by photolithography and Ar ion milling. Detailed fabrication process was described elsewhere.[19] The processed wafers were then annealed at 573 K in vacuum less than 1×10^{-4} Pa for an hour. SHE in these devices with various t_{HM} was measured at 305 K by means of SMR. For the measurements of SMR, the current, which is less than equal to 5 μA, is passed through the devices in the x-axis direction and external magnetic field between -4 and +4 Tesla is applied to the both y- and z-axes directions in inset of Fig. 2(c). For all films, the saturation magnetization (M_S) value of $Co_{20}Fe_{60}B_{20}$ is ~1.5 × 10^6 A/m. This value is nearly consistent with the nominal $Co_{20}Fe_{60}B_{20}$ saturation magnetization.[29] We also confirmed that the values of interfacial anisotropy (K_i) are nearly same value (about 1.45 [$\times10^{-3}$ J/m^2]) for (W/Hf)-multilayer/CoFeB/MgO systems with various t_W, which are much larger than that for β-W/CoFeB/MgO system. These K_i values are also consistent with previous results.[21] The reason of the nearly same K_i value for samples with various t_W would be originating from having the same interface structure of Hf(0.35)/CoFeB/MgO for the all (W/Hf)-multilayer/CoFeB/MgO systems prepared here.

III. STRUCTURAL FEATURE OF (W/Hf)-MULTILAYER/CoFeB/MgO STACK FILM

The film structure for (W(0.7)/Hf(0.35))$_5$/CoFeB(1.5)/MgO (1.0)/Ta(1.0) prepared by low- P_{Ar} condition was confirmed by high-resolution transmission electron microscopy (HR-TEM) image (Fig. 1(a)). Degree of the texture in MgO (1.0) layer for all systems prepared here were also investigated by reflection high energy electron diffraction (RHEED). As shown in Fig. 1(a), each film for (W(0.7)/Hf(0.35))-multilayer/CoFeB/MgO system is very flat. Figures 1(c)–1(e) show the typical RHEED patterns for MgO (1.0 nm) on CoFeB (3.0) in β-W (7.0)/CoFeB (3.0)/MgO (1.0) and (W (1.0)/Hf (0.35))$_5$ multilayer/CoFeB (3.0)/MgO (1.0) systems prepared in the conditions of high P_{Ar} and low P_{Ar}, respectively. Polycrystalline nature of MgO (1.0 nm) on CoFeB (3nm) was observed in the β-W (7nm) system (Fig. 1(c)). On the other hands, as shown in Figs. 1(d) and 1(e), the (100) oriented texture of MgO(1.0 nm) on CoFeB (3 nm) were observed in (W(1.0)/Hf(1.0))$_5$-multilayer systems prepared by high P_{Ar} and low P_{Ar}. This result is consistent with the HR-TEM images. Rough interface between β-W and CoFeB and not clear texture of MgO (1.0 nm) on CoFeB were observed in β-W (7)/CoFeB (1.5)/MgO (1.0) system from the HR-TEM images.[21] The degree of MgO(100) orientation is better for W/Hf-multilayer system prepared by low P_{Ar} condition (Fig. 1(e)) compared to the case of high P_{Ar} condition (Fig. 1(d)). The (100) oriented texture

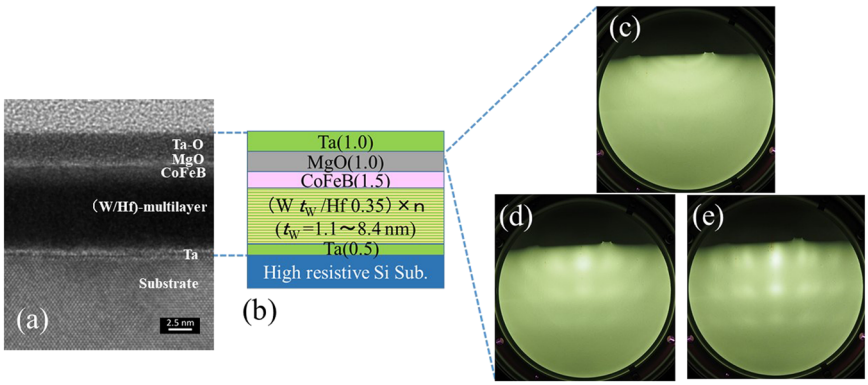

FIG. 1. (a) Cross-sectional transmission electron microscopy image for (W0.7/Hf0.35)-multilayer/CoFeB(1.5)/MgO(1.0)/Ta(1.0) system. (b) Cross-section view of the sputtered film stacks for artificial (W/Hf)-multilayer/CoFeB/MgO systems. The numbers in the parenthesis show the nominal thickness in nm. (c)-(e) are reflection high energy electron diffraction (RHEED) patterns of MgO (1.0) on CoFeB (3.0) for (c) β-W (7.0) and (W (1.0)/Hf (0.35))$_5$ multilayer systems prepared by (d) high Ar and (e) low Ar pressures.

© Author(s) 2021

of MgO(1.0 nm) were observed in the W thickness range of $t_W \leq 1.5$ and $t_W \leq 1.0$ for low P_{Ar} and high P_{Ar} conditions, respectively (not shown). This result indicates that the (W/Hf)-multilayer HM electrode is suitable for preparation of MgO (100) oriented magnetic tunnel junctions with high tunnel magnetoresistance properties.

IV. RESULTS OF ELECTRICAL PROPERTIES AND DISCUSSIONS

Figures 2(a) and 2(b) show the sheet conductance ($G_{xx} = L/(wR_{xx})$) as a function of the HM layer thickness (t_{HM}) in (W(h)/Hf)-multilayer and (W(l)/Hf)-multilayer systems, respectively, with reference result of β-W system,[21] which also show the result of β-W for comparison. The values of L and w in devices are $L = 205$ μm and $w = 5.1$ μm as shown in inset of Fig. 2(c). The W (h) and W (l) mean tungsten (W) films prepared at the high (h)-Ar-pressure (P_{Ar} =2.55 Pa) and low (l)-Ar-pressure (P_{Ar}=0.39 Pa) conditions, respectively. Since the slope in Figs. 2(a) and 2(b) is the inverse of the resistivity of HM ($1/\rho_{xx}$), we can see from Figs. 2(a) and 2(b) that the resistivity ρ_{xx} values for the all (W/Hf)-multilayer systems are smaller than that for β-W. As shown in Fig. 2(b), there are phase transition from amorphous phase to that containing α-phase W for the device with (W(l) (t_W)/Hf (0.35))-multilayer systems with t_W = 1.0 and 1.2 nm. The phase transition thicknesses (t_T) are $t_T \sim 3.9$, 3.8 nm for (W(l) (t_W)/Hf (0.35))-multilayer systems with t_W = 1.0 and 1.2 nm, respectively, whereas there is no anomaly for other devices. From here, we use the data of less than t_T in (W (l) (t_W)/Hf (0.35))-multilayer systems with t_W=1.0 and 1.2 nm for analyzing the value of ρ_{xx} and data of SMR for estimating the $|\theta_{SH}|$, σ_{SH} and spin diffusion length (λ_S). The values of the resistivity (ρ_{xx}) for (W(h) (t_W)/Hf (0.35))-multilayer (t_W = 0.35, 0.7, 1.0 nm) and (W(l) (t_W)/Hf (0.35))-multilayer (t_W = 0.35, 0.7, 1.0, 1.2 nm) systems as a function of W thickness (t_W) are shown in Fig. 2(c). The estimated value of ρ_{xx} for β-W obtained by the least-square-fit in Fig. 2(a) is also plotted in the Fig. 2(c) (red line). As shown in Fig. 2(c), the resistivity values for (W/Hf)-multilayer systems are smaller than that for β-W system and slightly decreases monotonically with increasing t_W (see the black solid line in Fig. 2(c)). We did not prepare (W(h) (1.2)/Hf (0.35))-multilayer system, because we could not observe MgO(100) texture in (W(h) (1.2)/Hf (0.35))$_5$ multilayer/CoFeB/MgO system (MgO has an amorphous structure). Because the metastable polycrystalline β-W has a higher resistance, amorphous W has a lower resistance compared to that of β-W. The ρ_{xx} values are nearly the same between artificially synthesized (W(h) (t_W)/Hf (0.35)) and (W(l) (t_W)/Hf (0.35))-multilayers prepared at P_{Ar}=2.55 Pa and P_{Ar}=0.39 Pa as shown in Fig. 2(c). This would because the multilayers have a same amorphous structure.

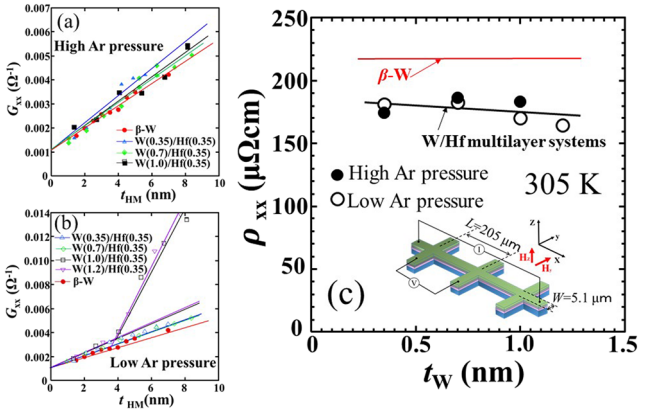

FIG. 2. (a) (b) show sheet conductance (G_{xx}) as a function of HM thickness (t_{HM}). The solid lines in (a) and (b) are linear fits to the data. (c) shows the estimated resistivity (ρ_{XX}) as a function of W thickness. The black solid line in (c) is the result of linear fit to the data and the red solid line in (c) is the plot of ρ_{xx} for β-W obtained by the least-square-fit in (a). Inset in (c) is schematic diagram of a prepared device.

Figures 3(a) and 3(b) show the typical longitudinal resistance (R_{xx}) versus external magnetic field (H) measured at 305 K for the devices with amorphous (W(h) (1.0)/Hf (0.35)) and amorphous (W(l) (1.0)/Hf (0.35))-multilayer systems, respectively. As shown in Figs. 3(a) and 3(b), the values of R_{xx} in the magnetic field directions along z-axis: $H_z > 0$ T and $H_z < 0$ T are nearly the same (for example, R_{xx} (H_z = 4 T) ~ R_{xx} (H_z = -4 T)), however, the values of R_{xx} in the magnetic field directions along y-axis: $H_y > 0$ T and $H_y < 0$ T are different from each other for the both devices with amorphous (W(h) (1.0)/Hf (0.35)) and amorphous (W(l) (1.0)/Hf (0.35))-multilayer systems. For both devices with amorphous (W (1.0)/Hf (0.35))-multilayers, the value of R_{xx} at H_y = 4 T is smaller than that at H_y = -4 T. These are related to the anomalous Nernst voltage (V_{Nernst}) due to the thermal hot electron current flow from the film to high resistive Si substrate as discussed in Ref. 19. The degree of the difference of R_{xx} values between for $H_y > 0$ T and $H_y < 0$ is smaller in the case of (W(l) (1.0)/Hf (0.35))-multilayer system compared with the case of (W(h) (1.0)/Hf (0.35))-multilayer systems. This would be related to the slight difference of the absolute value of R_{xx} for between (W(l) (1.0)/Hf (0.35)) and (W(h) (1.0)/Hf (0.35))-multilayers as shown in Figs. 3(a) and 3(b), because we flowed the same current value of I = 3 μA during measurements. The V_{Nernst} sign for amorphous W/Hf multilayers is the same with that for crystalline W systems.[19] Therefore, the current would mainly flow in the amorphous W in (W/Hf)-multilayer systems.

In order to neglect the anomalous Nernst effect to analyze the SMR, we define the SMR by[19,21]

$$\mathrm{SMR} = \Delta R_{XX}/R_{XX}^{H=0} = \left[\Delta R_{XX}^{1} + \Delta R_{XX}^{2}\right]/2R_{XX}^{H=0}, \quad (1)$$

$$\Delta R_{XX}^{1} = R_{XX}(H_y = -1.6\mathrm{T}) - R_{XX}(H_Z = -1.6\mathrm{T}), \quad (2)$$

$$\Delta R_{XX}^{2} = R_{XX}(H_y = +1.6\mathrm{T}) - R_{XX}(H_Z = +1.6\mathrm{T}), \quad (3)$$

where $R_{XX}^{H=0}$ is the longitudinal resistance at H = 0 T.

We used the values of R_{XX} at $|H|$ = 1.6 T, which is the saturation magnetic field value for CoFeB in the magnetic hard-axis direction, for the estimation of SMR, because we think that the slight increase in ΔR_{XX} with increasing $|H|$ above 1.6 T may originate from contribution of the Hanle magnetoresistance.[30,31]

© Author(s) 2021

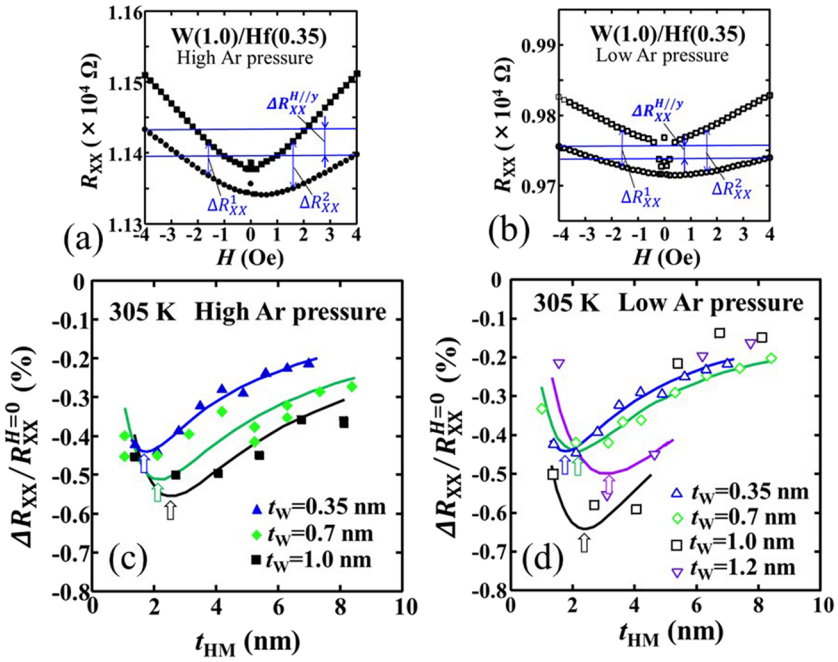

FIG. 3. Typical longitudinal resistance R_{xx} versus external magnetic field H oriented along the y axis (open and closed circles) and z axis (open and closed rectangulars) measured at 305 K for the device with (W(1.0)/Hf(0.35))-multilayers prepared (a) high and (b) low-Ar-pressures. SMR $\Delta R_{XX}/R_{XX}^{H=0}$ plotted against the HM layer thickness (t_{HM}) for (W/Hf)-multilayer systems prepared by (c) high Ar gas pressure and (d) low Ar gas pressure. The solid lines show the fitting results using drift diffusion model.

Figures 3(c) and 3(d) show the $\Delta R_{XX}/R_{XX}^{H=0}$ as a function of t_{HM} for (W(h) (t_W)/Hf (0.35))-multilayer systems (t_W = 0.35, 0.7, 1.0) and (W(l) (t_W)/Hf (0.35))-multilayer systems (t_W = 0.35, 0.7, 1.0, 1.2), respectively. The solid lines in Figs. 3(c) and 3(d) are the results fitted the measured data by using the equations:[22,26]

$$\mathrm{SMR} = \Delta R_{XX}/R_{XX}^{H=0} \sim \theta_{SH}^2 \frac{\lambda_S}{t_{HM}} \frac{\tanh(t_{HM}/2\lambda_S)}{1+\xi} \times \left[1 - \frac{1}{\cosh(t_{HM}/\lambda_S)}\right], \quad (4)$$

$$\xi \equiv \frac{\rho_{HM} t_{CoFeB}}{\rho_{CoFeB} t_{HM}}, \quad (5)$$

where λ_S is spin diffusion length and ρ_{CoFeB} = 139.9 $\mu\Omega$cm and ρ_{HM} are the resistivity estimated by the least-square-fitting shown in Figs. 2(a) and 2(b). As shown in Figs. 3(c) and 3(d), the thicknesses values of t_{HM} at which minimum magnitude of $\Delta R_{XX}/R_{XX}^{H=0}$ for the fitted solid lines in amorphous (W (t_W)/Hf (0.35))-multilayer systems with small t_W are thinner than those for thick t_W. This indicates the λ_S values in (W/Hf)-multilayers systems increase with increasing t_W in W (t_W)/Hf (0.35) multilayer systems. The applied SMR model is based on the drift diffusion model,[32] therefore the estimated θ_{SH} and the λs are all effective values. The magnitudes of $|\theta_{SH}|$ and λ_S of the amorphous (W/Hf)-multilayer HM electrodes are successfully obtained as shown next.

Figures 4(a)-4(c) show the results of the magnitudes of σ_{SH}, $|\theta_{SH}|$ and λ_S as functions of t_W and artificial-cycle-film thickness (t_{AFC} = t_W + 0.35 nm) for W/Hf multilayer systems. The estimated values of σ_{SH}, $|\theta_{SH}|$ and λ_S for β-W[21] are also plotted in the Figs. 4(a)-4(c) (red lines). A maximum magnitude in both σ_{SH} and $|\theta_{SH}|$ as a function of t_W are observed for (W (t_W)/Hf (0.35))-multilayer systems. Thus, we observed σ_{SH} values is 15% higher than the previous value,[21] when investing the t_W dependence detailly. As shown in Fig. 4(a), the all estimated values of σ_{SH} for (W/Hf)-multilayer systems are larger than that for β-W. This is due to the lower resistivity values for (W/Hf)-multilayer systems compared to that for β-W as shown in Fig. 2(c). The maximum magnitude of θ_{SH} value for amorphous (W (t_W)/Hf (0.35))-multilayer systems is -0.21 for t_W = 0.7, 1.0 nm. We found that the magnitude of $|\theta_{SH}|$ for amorphous (W/Hf)-multilayer systems with t_W = 0.7, 1.0 nm is nearly the same with that for β-W (θ_{SH} = -0.207) and found the decrease in $|\theta_{SH}|$ for t_W = 1.2 nm (θ_{SH} = -0.17).

As show in Fig. 4(c), we also found that the value of λs increases with increasing t_W. This would correlate with the t_{AFC} in amorphous (W (t_W)/Hf (0.35))-multilayer systems. The estimated value of λs in (W (1.2)/Hf (0.35))-multilayer system is nearly same with that in β-W (λs =1.05 nm) (red line in Fig. 4(c)). The low λs for (W/Hf)-multilayer systems with t_W = 0.35, 0.7, 1.0 would be related to the increase in the interfacial scattering of multilayer systems, and the nearly same in the λs for (W/Hf)-multilayer system with t_W = 1.2 would indicate the decrease in the interfacial scattering of multilayer systems due to the thick in W thickness. As shown in Figs. 4(a) and 4(b), it can be also seen that the spin-Hall effects (both σ_{SH} and $|\theta_{SH}|$) decrease at the film thickness where the scattering mechanism at the interface disappears (the t_{AFC} is thicker than equal to 1.2+0.35 nm ($t_{AFC} \geq$ 1.55 nm)). These results clearly suggest that artificially

© Author(s) 2021

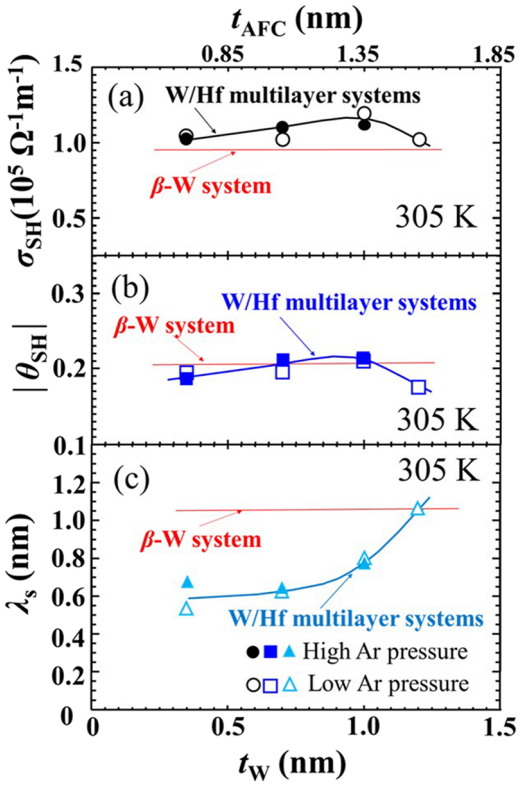

FIG. 4. (a) Estimated magnitude of the spin Hall conductivity (σ_{SH}) (open and closed black circles), (b) spin Hall angle $|\theta_{SH}|$ (open and closed blue rectangulars) and (c) spin diffusion length (λs) (open and closed light blue triangles) as functions of W thickness (tW) and artificial-cycle-film thickness (t_{AFC}) for the (W/Hf)-multilayer systems. The solid black and dark and light blue lines in (a)-(c) are guides for the eyes. The red solid lines in (a)-(c) are the plots of σ_{SH}, $|\theta_{SH}|$ and λs for β-W system.

synthesized multilayer system can enhance the spin-Hall effect and control the value of λs.

V. CONCLUSIONS

We prepared artificially synthesized (W/Hf)-multilayer/CoFeB/MgO systems and observed a maximum magnitude in spin Hall effect as a function of t_W in amorphous (W (t_W)/Hf (0.35))-multilayer systems. We found 15% enhancement of the magnitude of σ_{SH} by investigating the t_W dependence of spin Hall effect. In addition, we found that the value of λs correlates with the artificial-cycle-film thickness in (W (t_W)/Hf (0.35))-multilayer systems. These results clearly suggest that the artificially synthesized multilayer system can enhance the spin-Hall effect and control the value of λs. We also found that the degree of (100) oriented texture of MgO is higher for the artificially (W/Hf)-multilayer systems prepared by low Ar pressure condition, which would be better for preparation of MTJs with (W/Hf)-multilayer HM electrode in order to realize a high tunnel magnetoresistance resulting from coherent tunneling of Δ_1 electrons through the MgO (100) barrier. These results suggest that artificially synthesized multilayer system is one of the avenues for realizing spin devices using spin-orbit torque.

ACKNOWLEDGMENTS

This work was supported by the JST OPERA (JPMJOP1611) and JSPS KAKENHI (19H00844).

DATA AVAILABILITY

The data that support the findings of this study are available from the corresponding author upon reasonable request.

REFERENCES

[1] L. Liu, C.-F. Pai, Y. Li, H. W. Tseng, D. C. Ralph, and R. A. Buhrman, Science **336**, 555 (2012).
[2] G. Yu, P. Upadhyaya, Y. Fan, J. G. Alzate, W. Jiang, K. L. Wong, S. Takei, S. A. Bender, L.-T. Chang, Y. Jiang, M. Lang, J. Tang, Y. Wang, Y. Tserkovnyak, P. K. Amiri, and K. L. Wang, Nat. Nanotechnol. **9**, 548 (2014).
[3] W. Jiang, P. Upadhyaya, W. Zhang, G. Yu, M. B. Jungfleisch, F. Y. Fradin, J. E. Pearson, Y. Tserkovnyak, K. L. Wang, O. Heinonen, S. G. E. te Velthuis, and A. Hoffmann, Science **349**, 283 (2015).
[4] P. P. J. Haazen, E. Murè, J. H. Franken, R. Lavrijsen, H. J. M. Swagten, and B. Koopmans, Nat. Mater. **12**, 299 (2013).
[5] A. Chernyshov, M. Overby, X. Liu, J. K. Furdyna, Y. Lyanda-Geller, and L. P. Rokhinson, Nat. Phys. **5**, 656 (2009).
[6] I. M. Miron, K. Garello, G. Gaudin, P.-J. Zermatten, M. V. Costache, S. Auffret, S. Bandiera, B. Rodmacq, A. Schuhl, and P. Gambardella, Nature **476**, 189 (2011).
[7] J. Kim, J. Sinha, M. Hayashi, M. Yamanouchi, S. Fukami, T. Suzuki, S. Mitani, and H. Ohno, Nat. Mater. **12**, 240 (2013).
[8] S. Fukami, T. Anekawa, C. Zhang, and H. Ohno, Nat. Nanotechnol. **11**, 621 (2016).
[9] K.-S. Lee, S.-W. Lee, B.-C. Min, and K.-J. Lee, Appl. Phys. Lett. **104**, 072413 (2014).
[10] K. Garello, C. O. Avci, I. M. Miron, M. Baumgartner, A. Ghosh, S. Auffret, O. Boulle, G. Gaudin, and P. Gambardella, Appl. Phys. Lett. **105**, 212402 (2014).
[11] C. Zhang, S. Fukami, H. Sato, F. Matsukura, and H. Ohno, Appl. Phys. Lett. **107**, 012401 (2015).
[12] M.-H. Nguyen, C. F. Pai, K. X. Nguyen, D. A. Muller, D. C. Ralph, and R. A. Buhrman, Appl. Phys. Lett. **106**, 222402 (2015).
[13] S. Fukami, T. Anekawa, C. Zhang, and H. Ohno, Nat. Nanotechnol. **11**, 621 (2016).
[14] S. V. Aradhya, G. E. Rowlands, J. Oh, D. C. Ralph, and R. A. Buhrman, Nano Lett. **16**, 5987 (2016).
[15] M. Baumgartner, K. Garello, J. Mendil, C. O. Avci, E. Grimaldi, C. Murer, J. Feng, M. Gabureac, C. Stamm, Y. Acremann, S. Finizio, S. Wintz, J. Raabe, and P. Gambardella, Nanotechnol **12**, 980 (2017).
[16] Y. Kato, Y. Saito, H. Yoda, T. Inokuchi, S. Shirotori, N. Shimomura, S. Oikawa, A. Tiwari, M. Ishikawa, M. Shimizu, B. Altansargai, H. Sugiyama, K. Koi, Y. Ohsawa, and A. Kurobe, Phys. Rev. Appl. **10**, 044011 (2018).
[17] H. Honjo, T. V. A. Nguen, T. Watanabe, T. Nasuno, C. Zhang, T. Tanigawa, S. Miura, H. Inoue, M. Niwa, T. Yoshiduka, Y. Noguchi, M. Yasuhira, A. Tamakoshi, M. Natsui, Y. Ma, H. Koike, Y. Takahashi, K. Furuya, H. Shen, S. Fukami, H. Sato, S. Ikeda, T. Hanyu, H. Ohno, and T. Endoh, IEDM Tech. Dig. **28**, 5 (2019).
[18] M. Natsui, A. Tamakoshi, H. Honjo, T. Watanabe, T. Nasuno, C. Zhang, T. Tanigawa, H. Inoue, M. Niwa, T. Yoshiduka, Y. Noguchi, M. Yasuhira, Y. Ma, H. Shen, S. Fukami, H. Sato, S. Ikeda, H. Ohno, T. Endoh, and T. Hanyu, in 2020 Symposia on VLSI Technology and Circuits, CM2.2, 2020.
[19] Y. Saito, N. Tezuka, S. Ikeda, H. Sato, and T. Endoh, Appl. Phys. Exp. **12**, 053008 (2019).

© Author(s) 2021

[20]Y. Saito, N. Tezuka, S. Ikeda, H. Sato, and T. Endoh, AIP. Advances **9**, 125312 (2019).
[21]Y. Saito, N. Tezuka, S. Ikeda, H. Sato, and T. Endoh, Appl. Phys. Lett. **116**, 132401 (2020).
[22]J. Liu, T. Ohkubo, S. Mitani, K. Hono, and M. Hayashi, Appl. Phys. Lett. **107**, 232408 (2015).
[23]C.-F. Pai, L. Liu, Y. Li, H. W. Tseng, D. C. Ralph, and R. A. Buhrman, Appl. Phys. Lett. **101**, 122404 (2012).
[24]A. Ganguly, K. Kondou, H. Sukegawa, S. Mitani, S. Kasai, Y. Niimi, Y. Otani, and A. Barman, Appl. Phys. Lett. **104**, 072405 (2014).
[25]Y. Wang, P. Deorani, X. Qiu, J. H. Kwon, and H. Yang, Appl. Phys. Lett. **105**, 152412 (2014).
[26]J. Kim, P. Sheng, S. Takahashi, S. Mitani, and M. Hayashi, Phys. Rev. Lett. **116**, 097201 (2016).
[27]C. Zhang, S. Fukami, K. Watanabe, A. Ohkawara, S. DuttaGupta, H. Sato, F. Matsukura, and H. Ohno, Appl. Phys. Lett. **109**, 192405 (2016).
[28]L. Wang, R. J. H. Wesselink, Y. Liu, Z. Yuan, K. Xia, and P. J. Kelly, Phys. Rev. Lett. **116**, 196602 (2016).
[29]R. M. Bozorth, *Ferromagnetism* (Wiley-IEEE Press, New York, 1993).
[30]M. I. Dyakonov, Phys. Rev. Lett. **99**, 126601 (2007).
[31]S. Velez, V. N. Golovach, A. Bedoya-Pinto, M. Isasa, E. Sagasta, M. Abadia, C. Rogero, L. E. Hueso, F. S. Bergeret, and F. Casanova, Phys. Rev. Lett. **116**, 016603 (2016).
[32]V. P. Amin and M. D. Stiles, Phys. Rev. B **94**, 104420 (2016).

© Author(s) 2021